ISBN: 978-3-95450-132-8 doi:10.18429/JACoW-IPAC2014-MOPRI030

BASIC DESIGN OF A 20K C-BAND 2.6-CELL PHOTOCATHODE RF GUN*

T. Tanaka#, T. Sakai, K. Nakao, K. Nogami, M. Inagaki, LEBRA, Nihon University, Funabashi, Japan
T. Shintomi, ARISH, Nihon University, Tokyo, Japan
T. Takatomi, M. Yoshida, M. Fukuda, J. Urakawa, KEK, Ibaraki, Japan

Abstract

A cryo-cooled C-band photocathode RF gun that operates at 20K is under development. The RF gun is a 2.6-cell pillbox-type π-mode cavity with the resonant frequency of 5712 MHz. Using high-purity Oxygen-free copper, a high accelerating efficiency is expected from a theoretical prediction of the anomalous skin effect at low temperatures. Considering the cooling capacity, the RF gun system is designed to operate at the RF duty factor of 0.01%. After machining of the basic test cavity for low power and low temperature tests, the RF properties of the cavity have been measured at room temperature prior to assembling at KEK by means of diffusion bonding technique. Since it is intended for basic understanding and measurements of low temperature RF properties, the cavity has not been equipped with structures for the photocathode assembling or the RF input coupler. The measured properties of the cavity have shown good agreement with the results of Superfish simulation.

INTRODUCTION

A C-band photocathode RF gun is under development for future use in the compact X-ray linac developed at KEK [1]. The electron beam is extracted by using a cryo-cooled copper RF cavity, which can be driven with considerably low RF power compared to those in room temperature RF guns. As a basic design the RF gun cavity consists of 2.6-cell pillbox-type π-mode structure and operates at 5712 MHz under low temperature of 20K. A low power test cavity has been designed with Poisson Superfish [2] for basic understanding of the RF properties at low temperature. The low temperature experiment on the test cavity is under preparation. This paper reports the result of the RF properties measured at room temperature before diffusion bonding.

SPECIFICATIONS OF THE RF GUN

The surface resistance of the cavity material and resultant RF power efficiency of beam acceleration depend on the cavity temperature. The behavior of the surface resistance at 5712 MHz has been calculated on the basis of the theory of the anomalous skin effect [3], which is shown in Fig. 1 together with the result of calculation of the normal skin effect for comparison. In the calculation the copper material with a residual resistance ratio (RRR) of 3000 was assumed corresponding to the purity of more than 99.9999% (6N) that was specified for the fabrication of the cavity.

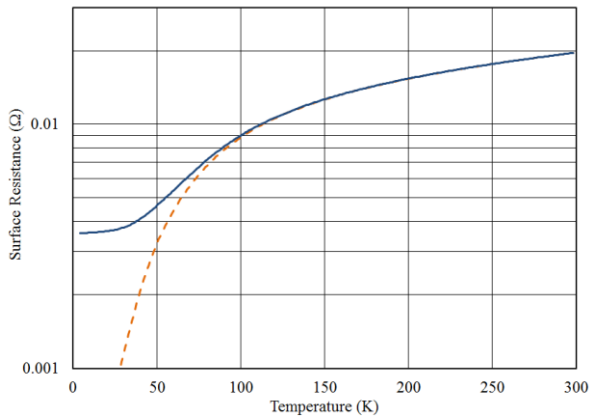

Figure 1: Temperature dependence of theoretical surface resistances of RRR=3000 copper cavity at 5712 MHz. Solid line: result of the anomalous skin effect, dashed line: the normal skin effect.

As seen in Fig. 1, the surface resistance of the cavity at 20K is reduced to approximately 18% of that at room temperature, which means that the quality factor of the cavity is 5.5 times as large as that at room temperature.

From the result of the calculation, the design specifications for the cryo-cooled copper RF gun cavity has been determined as listed in Table 1. The Q_0 and the shunt impedance expected at room temperature by

Table 1: Specifications for the 2.6-Cell 20K Cryo-cooled Photocathode RF Gun

RF frequency	5712	MHz
Source peak RF power	4	MW
Q_0	60000	
Shunt impedance	550	MΩ/m
Coupling coefficient	20	
Cavity length	68.2	mm
RF pulse duration	2	μs
Maximum field on axis	95	MV/m
Maximum peak RF loss	0.73	MW
Output beam energy	3	MeV
RF duty factor	0.01	%
Maximum beam charge	0.5	nC/bunch
Laser pulse repetition rate	357	MHz
Laser pulse length	10-20	ps

* Work supported by the Photon and Quantum Basic Research Coordinated Development Program of the Japanese Ministry of Education, Culture, Sports, Science, and Technology (MEXT).
# tanaka@lebra.nihon-u.ac.jp

ISBN: 978-3-95450-132-8 doi:10.18429/JACoW-IPAC2014-MOPRI030

Superfish calculation were approximately 11000 and 103 MΩ/m, which correspond to approximately 60000 and 550 MΩ/m, respectively at 20K. The build-up time of the RF field in the cavity should be sufficiently short compared to the RF pulse duration of 2 μs. This will be achieved by a large coupling coefficient at the RF input coupler. The maximum peak RF power loss in the cavity without beam load is 0.73 MW for the source power of 4 MW. Preliminary simulation of beam acceleration has shown that the electron beam with 0.5 nC/bunch is accelerated up to 3 MeV at less than 0.7 MW of peak RF power loss in the cavity, provided that the electron beam is extracted at a repetition rate of 357 MHz. At the operation with RF duty factor of 0.01%, the average cavity power loss of 73 W is removed through heat transfer media with two 50-W cryo-refrigerators.

FABRICATION OF TEST CAVITY

The RF gun cavity operates at a frequency of 5712 MHz under low temperature of 20K. On the other hand, machining of the test cavity elements and measurements of the RF properties should be carried out at room temperature. The dimensional change in the cavity between room temperature and 20K is more than 0.3%. Therefore, the estimation of the linear expansion ratio and the resultant change in the resonant frequency of the cavity is important in the determining of the final machining dimensions of the actual cavity.

The cavity machining temperature was assumed to be around 25°C. The expansion ratio of copper between 20K and 298K, L_{298}/L_{20} = 1.0033428, was deduced from the empirical approximate function for the linear thermal expansion coefficients given by NIST [4]. Employing the L_{298}/L_{20} ratio, the dimensions of the test cavity were corrected for the thermal expansion from 20K to 298K. Thus, the designed resonant frequency of the cavity at 298K in vacuum was 5692.970 MHz.

The cross-sectional view of a setup of the test cavity is shown in Fig. 2. There are no tuning structures in the cylinder walls. The holes with a diameter of 3.6 mm on the central axis at both the end-plates are for the bead-pull field measurement. The low power RF can be fed into the cavity with an antenna through either small hole located off-axis in the left-side end-plate, or through either hole on the axis of the end-plates. In addition to the setup in Fig. 2, other sets of a left-side end-plate with a different hole diameter and a 0.6-cell cylinder with a different

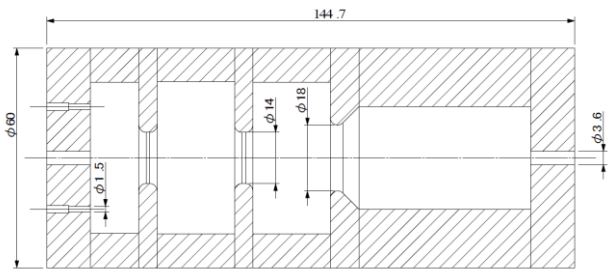

Figure 2: Cross-sectional view of the test cavity setup for field measurement prior to diffusion bonding.

inner diameter have been tested in order to check the accuracy of the Superfish calculation for the effect of the hole in the end-plate on the resonant frequency. In the actual RF gun cavity, the photocathode will be mounted at the center of the left side end-plate. The right half of the cavity was designed as part of the structure for a coaxial RF input coupler, which simply has a role as an RF cutoff tube in the present configuration. Due to difficulties in cooling the inner electrode of a coaxial coupler, however, a cylindrical waveguide will be employed in the advanced design in place of the right side tube in Fig. 2.

RF PROPERTIES BEFORE DIFFUSION BONDING

The RF properties of the test cavity have been measured under normal atmospheric conditions using a network analyzer E5071C (Agilent Technologies). The temperature, humidity and pressure of the air in the experimental room and the temperature of the cavity wall were recorded always during the measurements in order to convert every measured resonant frequency into that at a given condition. The conversion functions and relevant parameters implemented in the Superfish utility code Convertf were applied to this process.

Unperturbed π-mode Resonant Frequency

Though the actual machining temperature was 23.5°C, no corrections of cavity dimensions were made for the difference of 1.35°C from the assumed temperature of 24.85°C. Thus, the measured values of the resonant frequency have been converted to that at 23.5°C in vacuum and compared with the designed frequency of 5692.970 MHz. The temperature difference in machining can cause a frequency shift of approximately 128 kHz from 5712 MHz at 20K.

The unperturbed π-mode frequencies measured by replacing the set of the 0.6-cell cylinder and the left-side end-plate in Fig. 2 are listed in Table 2. In each set the frequency shift caused by the feeding antenna was eliminated by cutting gradually the antenna length inserted into the cavity until the resonant frequency became constant. The frequency of the same set measured after replacement with other sets has been reproduced roughly within errors of ±20 kHz. The results listed in Table 2 are the mean values of repeated measurement.

The result in Table 2 suggests that the frequency shift effect of the central holes in the end-plate have been well compensated for by adjusting the 0.6-cell cylinder

Table 2: π-mode Resonant Frequencies at Different Sets of 0.6-cell Cylinder and End-plate

cylinder diameter (mm)		holes in the end-plate	frequency (MHz)
designed	measured		
41.4322	41.4335	none	5692.47
41.4344	41.4339	ϕ2.0 mm	5692.58
41.4449	41.4457	ϕ3.6 mm	5692.50
41.4449	41.4557	ϕ3.6 mm + 2 x ϕ1.5mm	5692.47

ISBN: 978-3-95450-132-8 doi:10.18429/JACoW-IPAC2014-MOPRI030

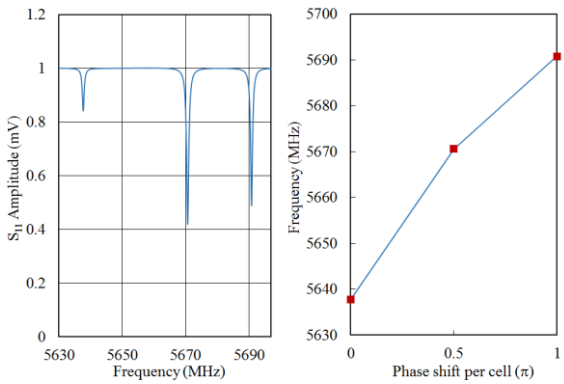

Figure 3: The resonance spectrum and the dispersion relation of the 2.6-cell cavity.

diameters with Superfish calculation. However, the frequencies are 400 to 500 kHz lower than the designed value. This discrepancy cannot be explained by the small machining errors in each element of the cavity. The result also suggests that the off-axis ϕ1.5 mm holes have negligibly small effect on the frequency.

The dispersion relation measured for the 2.6-cell cavity is shown in Fig. 3. The separation between the 1/2-π mode and the π mode frequencies is approximately 20 MHz consistent with which was predicted from the simulation by Superfish. The Q_0 value of the π mode resonance estimated from the Smith chart was 9015, which is expected to be higher after diffusion bonding.

Electric Field Distribution

The electric field distribution on the central axis of the 2.6-cell cavity has been analyzed from the bead-pull measurement using a metal sphere of 2 mm in diameter. The length of the antenna inserted into the cavity through one of the small off-axis holes in Fig. 2 was chosen so that the RF transmission peak at the resonant frequency was sufficiently significant for a good S/N ratio and the frequency shift was negligibly small. Figure 4 shows the picture of the cavity located on the test bench for bead-pull measurements. The result of the π mode field is shown in Fig. 5, where the frequency shifts were measured at 0.5-mm intervals over the entire length of the cavity. The field distribution obtained from the frequency shift data is shown in Fig. 6 together with the result of the simulation by Superfish. The r/Q ratio deduced from the distribution is 365 Ω, which is 3% lower than the result by Superfish.

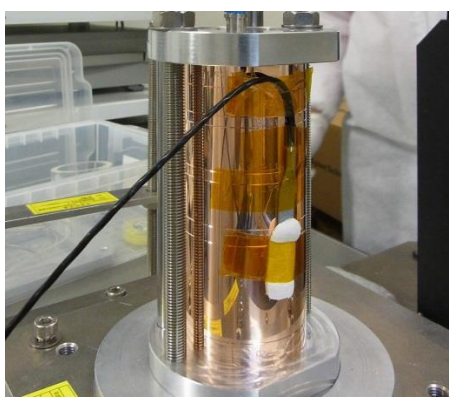

Figure 4: Picture of the 2.6-cell cavity on the test bench for bead-pull measurements.

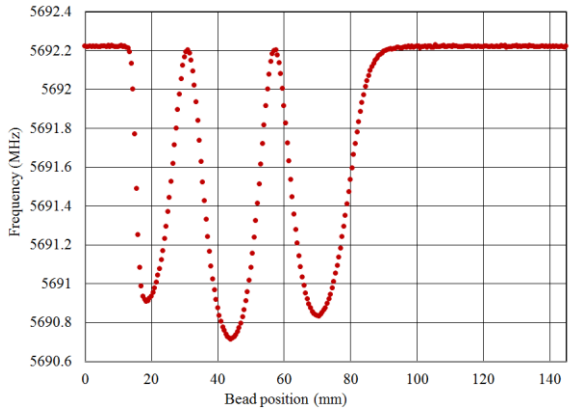

Figure 5: Shift of the π-mode resonant frequency in the bead-pull measurement.

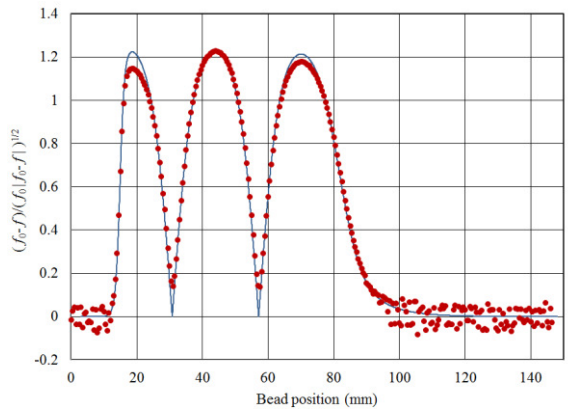

Figure 6: The π- mode electric field distribution. The solid line shows the result of simulation by Superfish.

CONCLUSIONS

The RF properties of the basic test cavity for the 2.6-cell C-band cryo-cooled photocathode RF gun have been measured at room temperature prior to diffusion bonding in KEK. Though the accelerating frequency has been 400-500 kHz lower than the designed value, other results are in agreement with the simulation by Superfish. The low power test at 20K and fabrication of the next test cavity with an RF coupler will be carried out in 2014.

REFERENCES

[1] M. Fukuda et al, NA-PAC13, Pasadena, September 2013, p. 589-591 (2013); http://www.JACoW.org
[2] J. H. Billen and L. M. Young, LA-UR-96-1834 (2006), Los Alamos National Laboratory.
[3] E. H. Reuter and E. H. Sondheimer, Proc. the Royal Society of London A, Mathematical and Physical Sciences, 195, 1042 (1948) 336-364.
[4] http://cryogenics.nist.gov/MPropsMAY/OFHC%20Copper/OFHC_Copper_rev.htm